IAI Journals.ASM.org

Chlamydia pneumoniae Infection Promotes Vascular Smooth Muscle Cell Migration through a Toll-Like Receptor 2-Related Signaling Pathway

Beibei Wang, Lijun Zhang, Tengteng Zhang, Haiwei Wang, Junxia Zhang, Junyan Wei, Bingling Shen, Xin Liu, Zhelong Xu, Lijun Zhang

Department of Pathophysiology, School of Basic Medical Sciences, Tianjin Medical University, Tianjin, China

The migration of vascular smooth muscle cells (VSMCs) from the media to the intima is proposed to be a key event in the development of atherosclerosis. Recently, we reported that *Chlamydia pneumoniae* infection is involved in VSMC migration. However, the exact mechanisms for *C. pneumoniae* infection-induced VSMC migration are not yet well elucidated. In this study, we examined the role of the Toll-like receptor 2 (TLR2) activation-related signaling pathway in VSMC migration induced by *C. pneumoniae* infection. An Affymetrix-based gene expression array was conducted to identify the changes of gene expression in rat primary VSMCs (rVSMCs) infected with *C. pneumoniae*. Both the microarray analysis and quantitative real-time reverse transcription (RT)-PCR revealed that TLR2 mRNA expression was strongly upregulated 12 h after *C. pneumoniae* infection. RT-PCR and Western blot analysis further showed that the expression levels of TLR2 mRNA and protein significantly increased at the different time points after infection. Immunocytochemical analysis suggested a TLR2 recruitment to the vicinity of *C. pneumoniae* inclusions. Cell migration assays showed that the TLR2-neutralizing antibody could significantly inhibit *C. pneumoniae* infection-induced rVSMC migration. In addition, *C. pneumoniae* infection stimulated Akt phosphorylation at Ser 473, which was obviously suppressed by the PI3K inhibitor LY294002, thereby inhibiting rVSMC migration caused by *C. pneumoniae* infection. Furthermore, both the infection-induced Akt phosphorylation and rVSMC migration were suppressed by the TLR2-neutralizing antibody. Taken together, these data suggest that *C. pneumoniae* infection can promote VSMC migration possibly through the TLR2-related signaling pathway.

Chlamydia pneumoniae is an obligate intracellular bacterium associated with respiratory tract infection. Moreover, atherosclerosis is a chronic inflammatory disease that develops in response to injury in the arterial wall (1), indicating that infectious agents may contribute to atherogenesis. Accumulating evidence indicates that the infection of *C. pneumoniae* could play a role in the initiation and progression of atherosclerosis (2, 3). However, how *C. pneumoniae* infection contributes to atherosclerosis remains unclear. The migration of vascular smooth muscle cells (VSMCs) from the media to the intima is regarded as a key event in the development of atherosclerosis. Understanding the mechanisms involved in VSMC migration and ultimately the development of strategies by which this process can be inhibited have been the major focuses of research.

Cell migration is believed to be under the control of complex regulatory mechanisms at multiple levels. Recently, *C. pneumoniae* infection has been shown to be involved in the migration of monocytes (2), HEp-2 cells (4), and VSMCs (5). The exact mechanisms of *C. pneumoniae* infection-induced VSMC migration have not yet been fully elucidated, although we have reported that *C. pneumoniae* infection promotes VSMC migration possibly through IQ domain GTPase-activating protein 1 (IQGAP1) (5). Therefore, further understanding of the mechanisms of *C. pneumoniae* infection-induced VSMC migration may provide important new evidence supporting the pathogenic role of *C. pneumoniae* in atherosclerosis.

Toll-like receptor 2 (TLR2) is a pattern recognition receptor that emerged as a critical component in the induction of innate immune and inflammatory responses (6, 7). TLR2 is expressed in most cardiovascular cells, including endothelial cells (8), VSMCs (9), and macrophages (10), and is thought to be essential in microbial detection and host cell activation. As a membrane surface receptor, TLR2 recognizes a variety of pathogens, including different bacteria and yeasts. Yang et al. found that TLR2 mRNA expression was upregulated when VSMCs were exposed to *C. pneumoniae* (9). Excitingly, TLR2 has been demonstrated to be able to mediate microvascular endothelial cell migration (11). TLR2 activation could result in the increases in the expressions of intercellular adhesion molecule 1, vascular cell adhesion molecule 1, and chemokines, thereby promoting neutrophil transendothelial migration (11, 12). In addition, TLR2 is also thought to have important effects on the starting procedure of the transmigration of polymorphonuclear leukocytes (13). Taken together, these studies indicate a close association of TLR2 with cell migration.

Akt, a serine threonine kinase known as protein kinase B, has been shown to play a significant regulatory role in cell migration (14). Akt activation is regulated primarily by phosphorylation at two sites: a conserved threonine residue (Thr 308) by phosphatidylinositol-dependent kinase 1 (PDK1) in the activation loop (15) and a serine residue (Ser 473) by PDK2 in the hydrophobic motif

Received 31 August 2013 **Accepted** 23 September 2013
Published ahead of print 30 September 2013
Editor: R. P. Morrison
Address correspondence to Lijun Zhang, lijunwz@hotmail.com.
B.W., L.Z., and T.Z. contributed equally to this work.

doi:10.1128/IAI.01087-13

(16). The receptor activator for the nuclear factor κB ligand was found to increase the migration of breast cancer cells by activating Akt (17). Lang et al. (18) reported that H_2O_2 elicited migration of VSMCs by activating the Akt signaling pathway. Activation of Akt has been shown in rat (19) and human aortic and coronary (20) VSMCs. Chan et al. (21) found that simvastatin-induced inhibition of VSMC migration involves the suppression of Akt activity. Recent evidence showed that stimulation of TLR2 activates the Akt signaling pathway (22, 23). Previous studies demonstrated that *C. pneumoniae* may stimulate or enhance innate immune and inflammatory response via TLR2, indicating a central role of TLR2 in *C. pneumoniae*-related cellular signaling (24, 25). Therefore, it is possible that activation of TLR2 could activate the Akt signaling pathway during *C. pneumoniae* infection. Whether the TLR2-related Akt signaling pathway mediates *C. pneumoniae* infection-induced VSMC migration is not well defined.

In the present study, we investigated the role of TLR2 in rat primary VSMC (rVSMC) migration induced by *C. pneumoniae* infection, examined the effects of *C. pneumoniae* infection on Akt activity in rVSMCs, and then explored the role of the activation of the TLR2-related signaling pathway in *C. pneumoniae* infection-induced VSMC migration.

MATERIALS AND METHODS

Antibodies. The following antibodies were used: primary mouse polyclonal anti-*C. pneumoniae* (CPN0308), which was kindly provided by Guangming Zhong (San Antonio, TX), goat polyclonal antibodies to TLR2 (Santa Cruz, CA), TLR2-neutralizing antibody (AbD Serotec, Kidlington, United Kingdom), rabbit anti-Akt and anti-phospho-Akt monoclonal antibodies (Ser 473) (Cell Signaling Technology, Beverly, MA), and mouse anti-β-actin monoclonal antibody (Beijing Zhongshan Goldenbridge Biotechnology Co., Ltd., Beijing, China). Secondary antibodies included rabbit anti-goat IgG labeled with Cy3 (Bioss, Beijing, China), rabbit anti-mouse IgG labeled with fluorescein isothiocyanate (FITC), donkey anti-goat IgG-horseradish peroxidase (HRP) (Santa Cruz, CA), goat anti-rabbit antibody IgG-HRP, and goat anti-mouse IgG-HRP (Jackson ImmunoResearch Laboratories, Inc., Pennsylvania, USA).

Infection of rVSMCs with *C. pneumoniae*. *C. pneumoniae* strain AR-39 (ATCC 53592) was propagated in HEp-2 cells (ATCC CCL-23) and purified by gradient centrifugation as described previously (26). Purified organisms were suspended in sucrose-phosphate-glutamic acid buffer, incubated for 1 h at 4°C, and stored at −80°C until use. The infectivity titers were determined by titration in HEp-2 cell monolayers (27). rVSMCs were prepared from the thoracic aorta of 8-week-old male Sprague-Dawley rats by the explant method and cultured in Dulbecco's modified Eagle's medium (DMEM) supplemented with 10% fetal bovine serum (FBS), 25 mg/ml vancomycin, and 10 mg/ml gentamicin as described previously (5). rVSMCs were seeded at a density of 3×10^5 cells/well into 6-well plates. Once confluent, the cells were serum starved for 12 h to achieve synchronous growth arrest. rVSMCs were then infected with 5×10^5 inclusion-forming units (IFU) (28). The plates were centrifuged at 1,700 × *g* for 50 min and then incubated at 37°C for 2 h. Subsequently, the medium was replaced with the culture medium with cycloheximide (2 μg/ml).

RNA isolation. Total RNA was isolated from *C. pneumoniae*-infected rVSMCs using the UNlQ-10 column-type total RNA extraction kit (Sangon, Shanghai, China) as described by the manufacturer. Degradation of the RNA was excluded by electrophoresis under RNase-free conditions, and the amount was quantified by spectrophotometry using Syngene GeneSnap (Bio-Rad, Hercules, CA).

Affymetrix gene chip. Starting with 10 μg of total RNA, samples were labeled and hybridized to the rat expression 230 2.0 arrays (Affymetrix, Santa Clara, CA) according to the manufacturer's protocol. Microarrays were scanned using the GeneChip Scanner 3000 7G (Affymetrix, Santa Clara, CA), and the raw data were extracted from the scanned images and initially analyzed for general assay quality using Affymetrix Microarray Suite software, version 5.0. CEL files were subsequently imported into the program RMAExpress (version 0.2 release) for global normalization and generation of expression values. Significance analysis was performed with the significance analysis of microarrays (SAM) algorithm (version 1.15).

Standard and quantitative RT-PCR. cDNA was prepared from RNA using 200 U of Moloney murine leukemia virus reverse transcriptase (TaKaRa, Otsu, Japan) according to a standard protocol. For standard PCR, the generated cDNA was amplified by PCR using specific primers: TLR2, 5′-GCTCTCCTGTTGTGCTTCTCCAC-3′ (forward) and 5′-CAG GAGCAGATGAAATGGTTGT-3′ (reverse) (29); GAPDH, 5′-AGTTCA ACGGCACAGTCAAG-3′ (forward) and 5′-TTGTCTGTGGGACACTG CTC-3′ (reverse). PCR was started at 95°C for 10 min, and subsequent amplification was performed as follows: for TLR2, 94°C for 15 s, 58°C for 15 s, and 72°C for 15 s for 30 cycles; for GAPDH, 94°C for 15 s, 60°C for 15 s, and 72°C for 15 s for 30 cycles and 72°C for 10 min in a microprocessor-driven thermal cycler (Eppendorf, Hannover, Germany). Following agarose gel electrophoresis of the standard PCR products, expression levels were determined semiquantitatively by densitometry. Quantitative real-time reverse transcription (RT)-PCR was performed with the ABI SDS 7500 system (Applied Biosystems). A 20-μl reaction mixture containing each primer and 1 μl of reverse-transcribed cDNA was prepared without changing the Mg^{2+} concentration. PCR conditions were as follows: after an initial denaturation step at 95°C for 30 s, 40 cycles of denaturation (95°C for 5 s), annealing, and synthesis (60°C for 34 s) were performed. The amount of each gene in each sample was relatively quantified using threshold cycle values.

Western blot analysis. Whole cellular protein in rVSMCs was obtained with the radioimmunoprecipitation assay (RIPA) lysis buffer (Beyotime, Haimen, China) for Western blot analysis. The aliquots were separated on SDS-PAGE (10%) and transferred to polyvinylidene fluoride membranes. Then, the membranes were blocked for 1 h at room temperature in Tris-buffered saline containing 5% nonfat dry milk and incubated overnight at 4°C with goat anti-TLR2 polyclonal antibody (1:200 dilution), rabbit anti-Akt monoclonal antibody (1:1,000 dilution), rabbit anti-phospho-Akt (Ser 473) monoclonal antibody (1:1,000 dilution), or mouse anti-β-actin monoclonal antibody (1:10,000 dilution). After being incubated with donkey anti-goat IgG-HRP (1:5,000 dilution), goat anti-rabbit IgG-HRP (1:10,000 dilution), or goat anti-mouse IgG-HRP (1:10,000 dilution), proteins were detected by an enhanced chemiluminescence kit (Beyotime, Haimen, China). The Western blot bands were scanned and semiquantified by densitometry.

Confocal microscopy. rVSMCs were plated onto 12-mm circular coverslips in 24-well plates (1.5×10^4 cells/well) and cultured overnight. After *C. pneumoniae* infection, cells were fixed with methanol and permeabilized with 0.1% Triton X-100 and then incubated for 3 h at 4°C with blocking buffer containing antibody against *C. pneumoniae* and antibody against TLR2. After being washed with phosphate buffer solution, cells were incubated with the corresponding secondary antibodies conjugated with FITC or Cy-3. Coverslips were washed three times, mounted with Prolong antifade (Molecular Probes, Pitchford, OR), and visualized on an LSM 510 confocal laser-scanning microscope (Zeiss, Thornwood, NY) by using LSM 510 software for image analysis.

Cell migration assays. Wound healing and Transwell migration assays were performed as previously described (5) with some modifications. Confluent cells were treated with serum-free medium containing hydroxyurea (Sigma, St. Louis, MO) for 12 h before the experiments were started (30). After incubation with hydroxyurea, 10 μg/ml of TLR2-neutralizing antibody (31) or 25 μM of the PI3K inhibitor LY294002 (Promega, Madison, WI) was added to the cells for 1 h.

For the wound healing assay, a single uniform scratch was carefully made using a sterile tip of a 200-μl yellow plastic pipette. After being carefully washed to remove the detached cells, cells were infected with *C.*

TABLE 1 Fold changes in the microarray for all 35 genes were found to be differentially regulated by *C. pneumoniae* infection and satisfied the comparison filtering criteria

Protein encoded by the gene	Gene name	NCBI RefSeq accession no.	Fold change
Proliferating cell nuclear antigen	*pcna*	NM_022381	2.34
Transforming growth factor, beta 3	*tgfb3*	NM_013174	−3.29
Chemokine (C-X3-C motif) ligand 1	*cx3cl1*	NM_134455	4.38
Early growth response 1	*egr1*	NM_012551	−3.51
Nuclear factor, interleukin 3 regulated	*nfil3*	NM_053727	−2.05
A kinase (PRKA) anchor protein 12	*akap12*	BG663107	−3.34
Inhibitor of DNA binding 2	*id2*	NM_013060	5.45
Coagulation factor III (thromboplastin, tissue factor)	*f3*	NM_013057	−4.59
Endothelin 1	*edn1*	NM_012548	−2.64
Chemokine (C-C motif) ligand 20	*ccl20*	AF053312	2.45
Stathmin-like 2	*stmn2*	BG668493	−2.25
Minichromosome maintenance complex component 6	*mcm6*	U17565	2.35
Protein kinase inhibitor, gamma	*pkig*	AA943815	−2.34
Phosphatidic acid phosphatase type 2B	*ppap2b*	AI177031	−2.56
Phosphoserine aminotransferase 1	*psat1*	AI230228	−2.16
ERBB receptor feedback inhibitor 1	*errfi1*	AI169756	−2.38
Gap junction protein, beta 2	*gjb2*	AI179953	−6.79
BAI1-associated protein 2	*baiap2*	BI279562	2.14
FBJ osteosarcoma oncogene	*fos*	BF415939	−20.99
		AI008792	4.68
Thrombomodulin	*thbd*	AA818521	−2.74
Similar to RIKEN cDNA 6330406I15	*rgd1307396*	AW916327	−2.26
RAS-like family 11 member B	*rasl11b*	BG375198	−2.9
Inhibitor of DNA binding 1	*id1*	M86708	2.3
Transforming growth factor alpha	*tgfa*	NM_012671	−2.2
NAD(P)H dehydrogenase, quinone 1	*nqo1*	J02679	2.6
Cd55 molecule	*cd55*	AB032395	−5.7
Similar to limb-bud and heart	*loc683626*	AA800701	−3.51
Minichromosome maintenance deficient 7 (*S. cerevisiae*)	*mcm7*	AI599678	2.17
Gremlin 2, cysteine knot superfamily, homolog (*Xenopus laevis*)	*grem2*	AA817956	2.57
Transforming growth factor alpha	*tgfa*	BG670310	−2.71
Toll-like receptor 2[a]	***tlr2***	**AW526982**	**2.21**
	rn.23094.2	AI548994	−3.32
Annexin A1	*anxa1*	AI236455	−2.46
Dual specificity phosphatase 1	*dusp1*	U02553	−2.79

[a] Bold type indicates the target gene examined by microarray analysis.

pneumoniae (at an infectious dose of 5×10^5 IFU). Multiple photographs of the wounds were then taken at 0 h and 24 h postwounding under an inverted Nikon microscope (Nikon Corporation, Tokyo, Japan) at a ×100 magnification. The areas of cell recoverage were determined with image analysis software (ImageJ). The ratio of the cellular recoverage area to the whole wound area was used to evaluate migration.

For the Transwell migration assay, rVSMCs were infected with *C. pneumoniae* for 14 h. Then, cells were seeded into the upper chamber of the Transwell inserts (1.5×10^4 cells per well) (Corning, St. Lowell, MA). Cells were subsequently allowed to migrate for 8 h at 37°C. The cells on the upper side of the inserts were softly scraped off. The cells that migrated to the lower side of the inserts were fixed with 4% paraformaldehyde and stained with 0.1% crystallin violet, and then the cells from nine independent, randomly chosen visual fields were counted in an inverted phase-contrast microscope (×200 magnification) for quantification of cells.

Statistical analysis. All experiments were repeated in triplicate, and all statistical analyses were performed using SPSS 16.0. Student's *t* test was used for the comparisons between two different groups. To compare between multiple experimental groups, one-way analysis of variance (ANOVA), followed by Tukey's *post hoc* analysis, was performed. The results were considered statistically significant at a *P* value of <0.05.

RESULTS

***C. pneumoniae* stimulates TLR2 expression in rVSMCs.** To explore whether *C. pneumoniae* infection could upregulate TLR2 mRNA expression in rVSMCs, a microarray was performed to assess the gene expression in rVSMCs 12 h after infection. Of the 31,042 transcripts (28,000 well-characterized genes) presented on the chips, 35 genes were found to be differentially regulated by *C. pneumoniae* infection and satisfied the comparison filtering criteria. Among them, 23 genes were downregulated and 12 were upregulated, including the TLR2 gene (2.21-fold change) (Table 1). The change of TLR2 mRNA expression was confirmed by TaqMan quantitative real-time RT-PCR (Fig. 1A) by using the same RNA samples that had been used for the microarray assay in the same manner and at the same time points. The changes in the expression levels of the validated genes showed the similar patterns in microarray and real-time RT-PCR 12 h after the infection.

To further examine the effects of *C. pneumoniae* infection on TLR2 expression, the standard PCR was performed to determine the expression levels of TLR2 mRNA at different time points in the

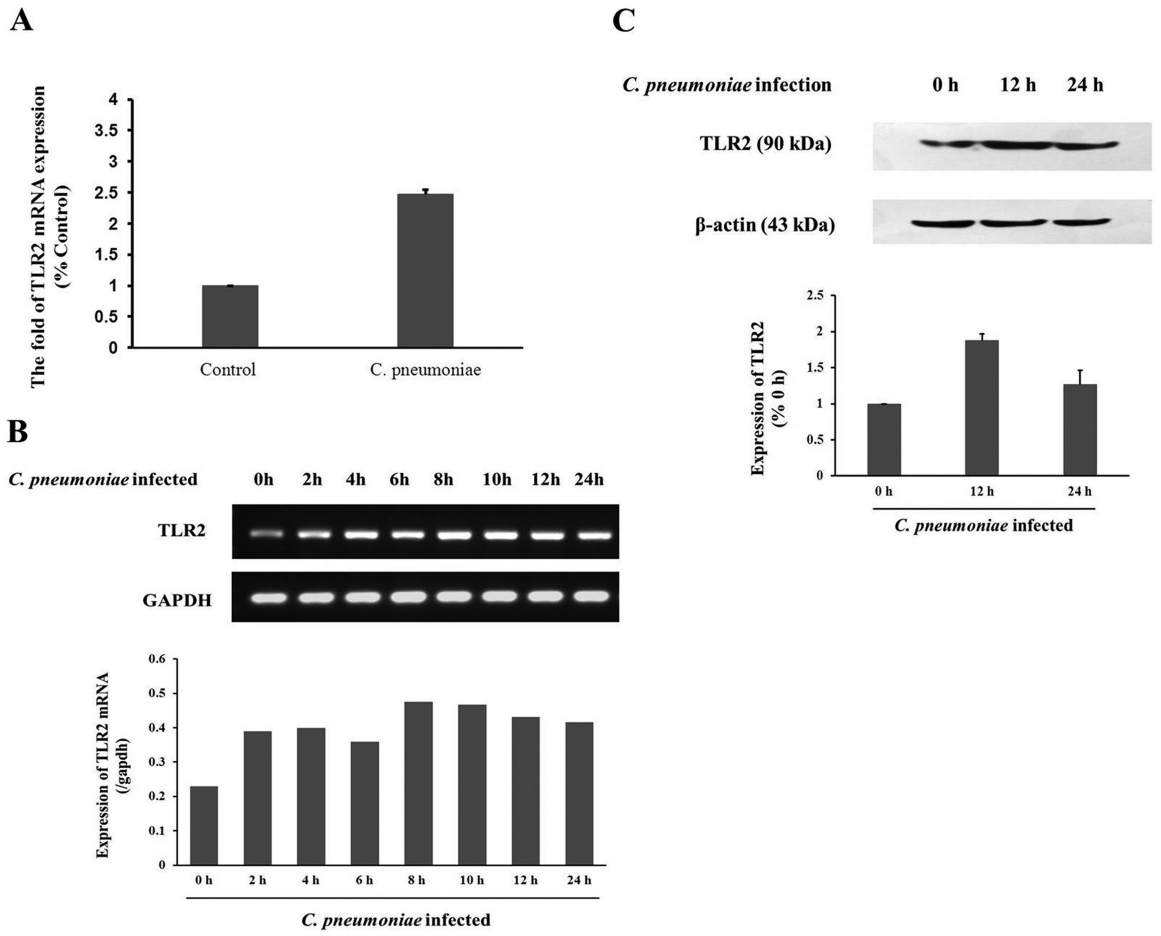

FIG 1 *C. pneumoniae* stimulates TLR2 expression in rVSMCs. (A) Validation of TLR2 gene expression profiling using quantitative real-time RT-PCR normalized to GAPDH expression. Data shown are mean values of PCR replicates from individual groups. (B) TLR2 mRNA expression at the indicated time points after *C. pneumoniae* infection. rVSMCs infected with *C. pneumoniae* (5×10^5 IFU) for 2 h, 4 h, 6 h, 8 h, 10 h, 12 h, and 24 h or control cells were lysed to prepare the total RNA. cDNA was amplified for 30 cycles, and PCR products were separated by agarose gel electrophoresis. Relative TLR2 mRNA expression levels determined by standard PCR ($n = 3$ replicates per group). (C) *C. pneumoniae* infection stimulates TLR2 protein expression in rVSMCs. Cells were infected with *C. pneumoniae* for 0 h, 12 h, or 24 h. Cell lysates were separated by SDS-PAGE, and blots were probed with anti-TLR2 and anti-β-actin antibodies, followed by donkey anti-goat IgG-HRP and goat anti-mouse IgG-HRP antibodies, and developed with enhanced chemiluminescence (ECL).

infected rVSMCs. TLR2 expression was detected 0 h, 2 h, 4 h, 6 h, 8 h, 10 h, 12 h, and 24 h after *C. pneumoniae* infection. The amount of TLR2 mRNA 2 h after infection roughly doubled compared to that of the control group and reached the peak at 8 h postinfection, with a prolonged expression until 24 h after *C. pneumoniae* infection (Fig. 1B). To confirm this finding, TLR2 protein levels were determined with Western blot analysis in *C. pneumoniae*-infected rVSMCs. As shown in Fig. 1C, the expression levels of the TLR2 protein were increased significantly 12 h and 24 h after *C. pneumoniae* infection. TLR2 protein expression at 12 h postinfection was higher than that seen 24 h after infection, and there was no significant difference between the two groups.

***C. pneumoniae*-infected rVSMCs recruit TLR2 around the inclusions.** To analyze the subcellular localization of TLR2 in rVSMCs infected with *C. pneumoniae*, the immunocytochemistry analysis was performed. Under fluorescence confocal microscopy, a scattered cytoplasmic distribution of TLR2 without a specific pattern was apparent in noninfected rVSMCs. In contrast, in *C. pneumoniae*-infected rVSMCs, large cytoplasmic inclusions were observed, and the expression of TLR2 was increased, especially around the *C. pneumoniae* inclusions (Fig. 2).

TLR2 mediates *C. pneumoniae* infection-induced rVSMC migration. Cell migration assays were performed to assess whether TLR2 was involved in *C. pneumoniae* infection-induced rVSMC migration. In the wound healing assay, *C. pneumoniae* infection accelerated the rVSMC migration velocity compared with that of the control group 24 h after the cell monolayer was scratched with a pipette tip (0.913 ± 0.031 compared to 0.623 ± 0.040, $P < 0.05$). Compared with *C. pneumoniae*-infected rVSMCs, the cell migration velocity was significantly reduced after the use of a TLR2-neutralizing antibody (10 μg/ml) (0.913 ± 0.031 compared to 0.763 ± 0.057, $P < 0.05$) (Fig. 3A). In addition, the Transwell migration assay showed that the number of rVSMCs infected with *C. pneumoniae* that migrated through the membrane was greater than that of the control group (55.32 ± 7.72 cells/view compared to 33.92 ± 5.96 cells/view, $P < 0.05$). The TLR2-neutralizing antibody markedly suppressed *C. pneumoniae* infection-induced rVSMC migration compared with that of the *C.*

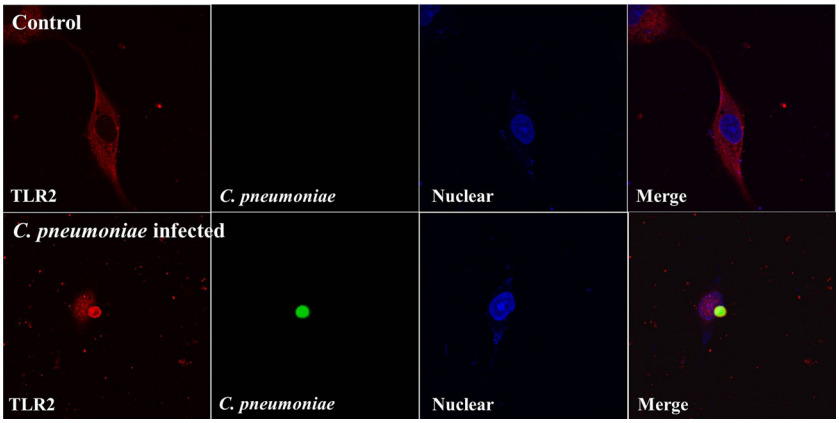

FIG 2 Confocal microscopy analysis of the TLR2 expression pattern in *C. pneumoniae*-infected rVSMCs. rVSMCs were grown in coverslips and infected with *C. pneumoniae* for 60 h and then were fixed, permeabilized, and stained using specific antibodies. *C. pneumoniae* inclusions were observed using a mouse polyclonal antibody to *C. pneumoniae*. Fluorescence micrographs were stained with TLR2-specific antibody. Cell nucleus was stained with DAPI (4′,6-diamidino-2-phenylindole).

pneumoniae infection group (36.95 ± 6.27 cells/view compared to 55.32 ± 7.72 cells/view, $P < 0.05$) (Fig. 3B).

***C. pneumoniae* infection induces Akt phosphorylation in rVSMCs.** Phosphorylation of Akt is critical for its effects on cell migration. Accordingly, we determined whether *C. pneumoniae* infection induces Akt phosphorylation in rVSMCs. As shown in Fig. 4, there was no significant difference in levels of total Akt protein expression between the control and *C. pneumoniae*-infected rVSMCs, whereas the level of Akt phosphorylation at Ser 473 was increased significantly at different time points after *C. pneumoniae* infection. The amount of phosphorylated Akt began to increase at 0.5 h after infection and reached the peak at 1 h postinfection, with a prolonged high level of Akt phosphorylation, and then decreased at 12 h and 24 h after infection (Fig. 4).

Suppression of Akt phosphorylation inhibits *C. pneumoniae* infection-induced rVSMC migration. To further address the significance of Akt phosphorylation in *C. pneumoniae* infection-in-

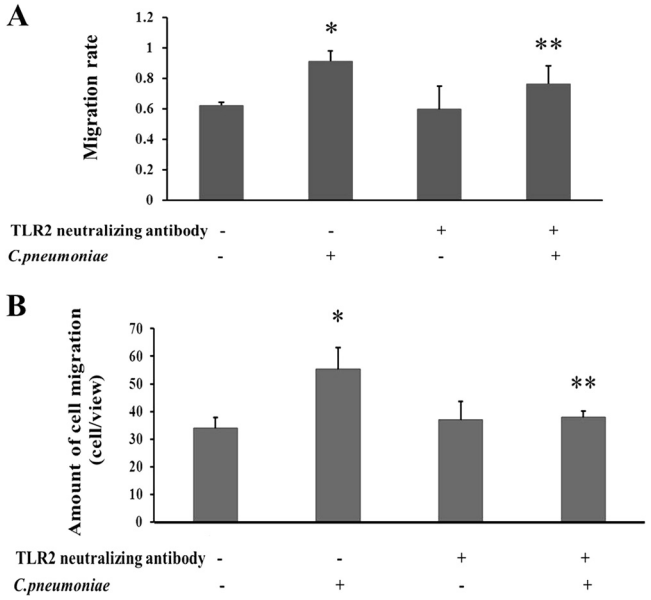

FIG 3 Effects of TLR2 on rVSMC migration induced by *C. pneumoniae* infection. The TLR2-neutralizing antibody was added 1 h before *C. pneumoniae* infection. (A) Wound healing assay. "Scratch wounds" were created by scraping the confluent cell monolayer with a sterile pipette tip, and then cells were infected with *C. pneumoniae* at an infectious dose of 5×10^5 IFU. Photographs were taken of the same wounded area of each well at 0 h and 24 h. The scratched regions were photographed under an inverted Nikon microscope (×100 magnification) at 24 h after *C. pneumoniae* infection. Migration velocity is presented as a ratio of the cellular recoverage area to the whole wound area. *, $P < 0.05$ versus control; **, $P < 0.05$ versus *C. pneumoniae* infection group. (B) Transwell migration assay. Cell morphology was observed by staining with 0.1% crystallin violet. The number of cells that had migrated through the pores was quantified by counting nine independent visual fields using a microscope (×200 magnification). *, $P < 0.05$ versus control; **, $P < 0.05$ versus the *C. pneumoniae* infection group.

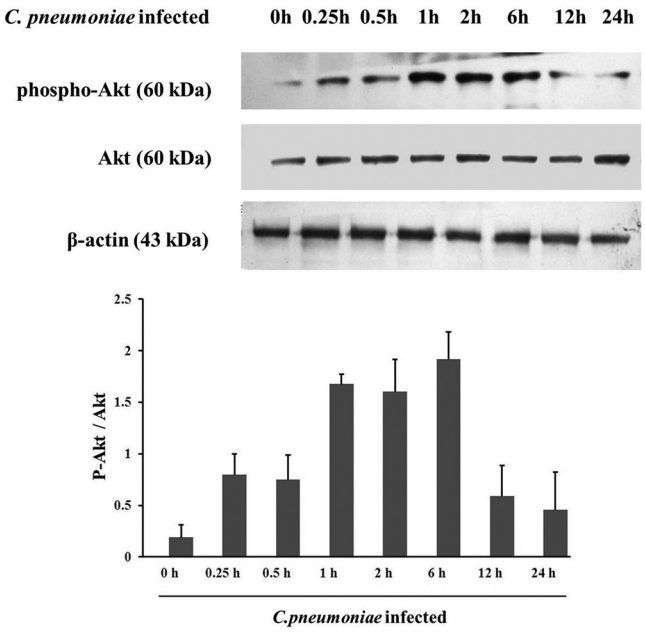

FIG 4 *C. pneumoniae* infection induces Akt phosphorylation in rVSMCs. Cells were infected with *C. pneumoniae* (5×10^5 IFU) for 0 h, 0.25 h, 0.5 h, 1 h, 2 h, 6 h, 12 h, or 24 h. Equal amounts of protein lysates were subjected to SDS-PAGE, and blots were probed with anti-Akt, anti-phospho-Akt (Ser 473), and anti-β-actin antibodies, followed by goat anti-rabbit IgG-HRP and goat anti-mouse IgG-HRP antibodies, and developed with ECL. P-Akt indicates phosphorylated Akt.

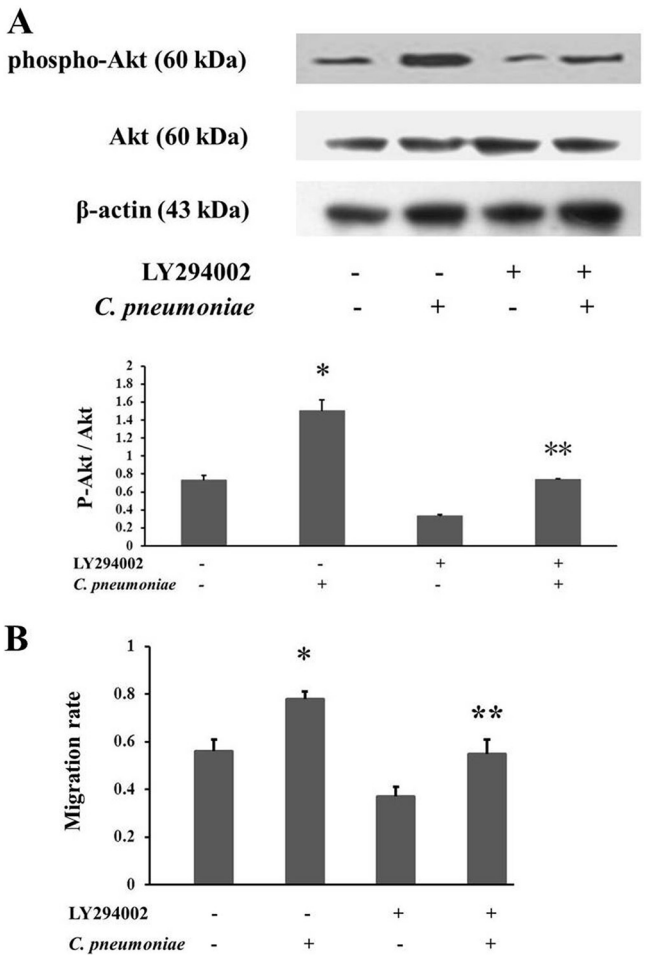

FIG 5 Suppression of Akt phosphorylation inhibits *C. pneumoniae* infection-induced rVSMC migration. (A) LY294002 (a phosphoinositide 3-kinase inhibitor) inhibits Akt phosphorylation induced by *C. pneumoniae* infection. After pretreatment with or without LY294002 (25 μM) at 37°C for 1 h, rVSMCs were inoculated with *C. pneumoniae* (5×10^5 IFU) and incubated for 2 h. Equal amounts of protein lysates were subjected to SDS-PAGE, and blots were probed with anti-Akt, anti-phospho-Akt (Ser 473), and anti-β-actin antibodies, followed by the corresponding HRP-conjugated secondary antibodies, and developed with ECL. P-Akt indicates phosphorylated Akt. (B) Effects of Akt phosphorylation on *C. pneumoniae* infection-induced rVSMC migration. After pretreatment with or without LY294002 (25 μM) at 37°C for 1 h, rVSMCs were inoculated with *C. pneumoniae* at an infectious dose of 5×10^5 IFU and incubated for 14 h. Cells were then incubated at 37°C for 10 h to allow cells to migrate through the membrane. Migration velocity is presented as a ratio of the cellular recoverage area to the whole wound area. *, $P < 0.05$ versus control; **, $P < 0.05$ versus the *C. pneumoniae* infection group.

duced rVSMC migration, we blocked the phosphorylation of Akt by the use of the PI3K inhibitor LY294002 (32) (1.50 ± 0.123 compared to 0.74 ± 0.009, $P < 0.05$) (Fig. 5A), and then the changes in cell migration were observed in the *in vitro* model of rVSMC monolayer wounding and restitution. The results showed that exposure to *C. pneumoniae* contributed to the acceleration of the wound closure (0.783 ± 0.034 compared to 0.557 ± 0.062, $P < 0.05$). Furthermore, the infection-induced rVSMC migration was markedly inhibited after the suppression of Akt phosphorylation by LY294002 compared with the cells infected only with *C. pneumoniae* (0.562 ± 0.052 compared to 0.783 ± 0.034, $P < 0.05$) (Fig. 5B).

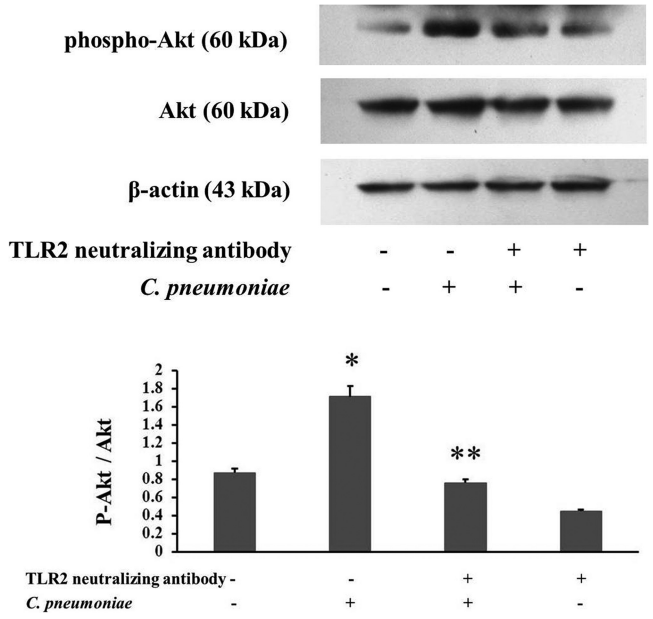

FIG 6 The TLR2-neutralizing antibody suppresses Akt phosphorylation induced by *C. pneumoniae* infection. rVSMCs cultured for 24 h in 6-well plates were incubated with the TLR2-neutralizing antibody (10 μg/ml) and then infected with *C. pneumoniae*. Equal amounts of protein lysates were subjected to SDS-PAGE, and blots were probed with anti-Akt, anti-phospho-Akt (Ser 473), and anti-β-actin antibodies, followed by the corresponding horseradish peroxidase-conjugated secondary antibodies, and developed with ECL. P-Akt indicates phosphorylated Akt. *, $P < 0.05$ versus control; **, $P < 0.05$ versus the *C. pneumoniae* infection group.

TLR2-neutralizing antibody suppresses Akt phosphorylation induced by *C. pneumoniae* infection. To analyze whether TLR2 mediates the promoting effect of *C. pneumoniae* infection on VSMC migration by activating Akt, we blocked TLR2 function using the TLR2-neutralizing antibody to determine the involvement of Akt in the TLR2 signaling pathway during *C. pneumoniae* infection. Western blot analysis showed that the elevated Akt phosphorylation level induced by *C. pneumoniae* infection was suppressed by the TLR2-neutralizing antibody (2.03 ± 0.251 compared to 2.96 ± 0.15, $P < 0.05$) (Fig. 6).

DISCUSSION

Despite the close link between *C. pneumoniae* infection and atherosclerosis (2, 5), the exact mechanisms by which *C. pneumoniae* infection may lead to the development of atherosclerosis is still not well understood. VSMC migration is known to be an essential element in the development of atherosclerotic lesions. Previous studies have found that *C. pneumoniae* infection can indirectly induce the transendothelial migration of neutrophils and monocytes by stimulating human coronary artery endothelial cells to secrete chemokines and adhesion molecules (33, 34). Recently, Schmidt et al. found that *C. pneumoniae* infection can directly induce monocyte migration through Matrigel (2). In addition, we have reported previously that *C. pneumoniae* infection can also directly promote the migration of HEp-2 cells (4) and VSMCs (5). Our previous study revealed that *C. pneumoniae* infection-induced VSMC migration may contribute to the upregulation of IQGAP1 expression (5). However, how *C. pneumoniae* infection regulates IQGAP1 remains unknown. Since IQGAP1 is only one

of the cytoskeletal regulatory proteins, it is reasonable to hypothesize that *C. pneumoniae* interacts with more than one of the key intracellular proteins involved in cell migration, especially the proteins required for recognizing *C. pneumoniae* and transmitting signals.

As a possible pattern recognition receptor for *C. pneumoniae*, TLR2 has also been shown to affect cell migration (13). However, whether TLR2 participates in VSMC migration caused by *C. pneumonia* infection is still unclear. To explore the potential mechanism involved in the infection-induced VSMC migration, microarray assay, RT-PCR, and Western blotting were performed to observe the effects of *C. pneumonia* infection on TLR2 mRNA and protein expressions. Our data showed that TLR2 mRNA expression was markedly upregulated in *C. pneumoniae*-infected rVSMCs compared with that in the control, which is consistent with the results reported by Yang et al. (9), who found that intracellular TLR2 may be responsible for the initiation of signal transduction events during *C. pneumoniae* infection. The expression of TLR2 mRNA began to increase within 2 h after *C. pneumoniae* infection, with a maximum 8 h after the infection, and was sustained for 24 h after the infection. Likewise, TLR2 protein expression levels were found to be significantly upregulated 12 h and 24 h after the infection, suggesting that the rapid effects of *C. pneumoniae* exposure and the persistent responses to *C. pneumoniae* infection in rVSMCs are both mediated by TLR2. These results also indicate that the expression of TLR2 in rVSMCs may mediate cellular responses to *C. pneumoniae* components at a posttranscriptional level.

We found that *C. pneumoniae* infection not only upregulated the expression level of TLR2 but also changed the TLR2 subcellular localization by promoting translocation of TLR2 to the vicinity of the inclusions. Similar results were observed in prostate epithelial cells infected by *Chlamydia muridarum* (35). Previous studies revealed that *C. pneumoniae* is taken up into cellular hosts within 2 h after cells were exposed to the elementary bodies (36). The cytokines are also released from the infected cells in a TLR2-dependent manner at 24 h postinfection (25, 37). Our data showed that the infected rVSMCs actively recruited TLR2 around the intracellular chlamydial inclusion, implying that TLR2 can recognize *C. pneumoniae* and is responsible for the initiation of signal transduction events upon infection with *C. pneumoniae*.

Recently, much interest has focused on the adaptive role of TLR2 as a key mediator of the innate immune response, inducing synthesis of antimicrobial peptides and cytokines that promote adaptive immunity. In fact, TLR2 activation may not only induce inflammatory responses that lead to pathogenic conditions but also be associated with cell migration (11, 38). Accordingly, we investigated the role of TLR2 in *C. pneumoniae* infection-induced rVSMC migration. In this study, we found that *C. pneumoniae* infection may promote VSMC migration by upregulating the expression of TLR2. In addition, the suppression of TLR2 activity with the TLR2-neutralizing antibody significantly inhibited cell migration induced by *C. pneumoniae* infection, suggesting a critical role of TLR2 activation in *C. pneumoniae* infection-induced VSMC migration. Others have also reported that TLR2 signaling in the airway may initiate cleavage of transmembrane junctional proteins to accommodate transmigration of recruited polymorphonuclear leukocytes (13). Moreover, TLR2 was shown to play an important role in the migration of cancer cells as well by stimulating the production of mitogen-activated protein kinase and inhibitor of kappaB kinase, and the blocking of TLR2 activity can attenuate metastasis of the tumor (39, 40). The activated TLR2 can stimulate cell migration not only indirectly by inducing proinflammatory cytokine expression (11, 12) but also directly by activating the intracellular dynamical system (41, 42). Activation of TLR2 may initiate the TLR2-MyD88-Rac1 signaling pathway, which accounts for the molecular mechanism of oxidative stress-induced migration of endothelial cells (39). Lasunskaia et al. (42) demonstrated that morphological cell rearrangements leading to the spreading and polarization of macrophages known to be important for cell migration were mediated by TLR2-dependent PI3K activation. Our previous study suggested a positive role of IQGAP1 in the regulation of VSMC migration induced by *C. pneumoniae* infection (5). How TLR2 transmits the signals from the membrane receptor to the cell migration-related downstream effectors after *C. pneumoniae* infection needs further studies.

Akt is known as a key regulator for many signal transduction pathways, modulating multiple cellular functions, including cell migration (43, 44). However, little is known about the role of Akt activation in the promotive effect of *C. pneumoniae* infection on the migration of VSMCs. In this study, we found that *C. pneumoniae* infection induced Akt phosphorylation at Ser 473 in rVSMCs at different time points after infection. Coombes and Mohony (36) found that Akt phosphorylation at Ser 473 was also detected for the duration of the experiment (2 h) after the addition of *C. pneumoniae* to the cells. Recently, *C. pneumoniae* infection has been shown to induce Akt phosphorylations at Thr 308 and Ser 473 (45). These studies suggest that *C. pneumoniae* infection can increase the level of phosphorylated Akt, partially supporting our findings. In contrast, Lin et al. (46) demonstrated that after 6 h of incubation with GroEL1, heat shock protein 60 of *C. pneumoniae*, Akt phosphorylation was significantly decreased in human coronary artery endothelial cells. Additional studies are needed to explain these contradictory data about the effects of *C. pneumoniae* infection on Akt phosphorylation.

To further determine the role of Akt phosphorylation in VSMC migration induced by *C. pneumoniae* infection, we first used the PI3K inhibitor LY294002 to suppress Akt phosphorylation (32) and then investigated the changes in the migration of rVSMCs by the wound healing assay. Our data showed that *C. pneumoniae* infection-induced rVSMC migration was significantly inhibited by the pretreatment of rVSMCs with LY294002, indicating that Akt phosphorylation plays an important role in VSMC migration stimulated by *C. pneumoniae* infection. LY294002 can also inhibit fibroblast growth factor 2-stimulated migration of the periodontal ligament cells through suppressing Akt activation (32). Recently, Walker et al. (47) reported that transforming growth factor β3 significantly induced motility of human prostate cancer PC3 cells by increasing the level of phosphorylated Akt (Ser 473), and LY294002 blocked transforming growth factor β3-stimulated migration via the suppression of Akt phosphorylation at Ser 473. These studies revealed that Akt phosphorylation is closely associated with cell migration, supporting our hypothesis that *C. pneumoniae* infection promotes VSMC migration possibly by inducing Akt phosphorylation.

The Akt pathway has been shown to be involved in TLR2 signaling (22, 23). Whether Akt activation participates in TLR2-mediated promoting effects of *C. pneumoniae* infection on VSMC migration remains unknown. Therefore, we blocked TLR2 function using the TLR2-neutralizing antibody to determine the in-

volvement of Akt in the TLR2 signaling pathway during *C. pneumoniae* infection. Excitingly, we found that Akt phosphorylation induced by *C. pneumoniae* infection was suppressed by the TLR2-neutralizing antibody, suggesting a partial dependence of Akt activation on TLR2. In the present study, we first demonstrated that *C. pneumoniae* infection-induced Akt phosphorylation was partially regulated by TLR2, although Akt activation has been shown to be involved in the TLR2 signaling pathway in *Listeria monocytogenes* (48) and mycobacteria (43). We have reported that *C. pneumoniae* infection may promote the migration of VSMCs by upregulating the IQGAP1 expression (5). Chen et al. (49) found that IQGAP1 can promote cell proliferation by Akt activation, suggesting that IQGAP1 is closely associated with Akt activation. Whether *C. pneumoniae* infection promotes VSMC migration through IQGAP1 activated by the TLR2-related Akt signaling pathway remains to be addressed.

In conclusion, we have demonstrated that *C. pneumoniae* infection can promote rVSMC migration possibly through the TLR2-related signaling pathway. Our data suggest the positive roles of TLR2 and Akt phosphorylation in the regulation of *C. pneumoniae* infection-induced VSMC migration, providing new evidence to support the hypothesis that *C. pneumoniae* infection accelerates the development of atherosclerosis by stimulating VSMC migration from the media to the intima, possibly through activating the TLR2-related signaling pathway.

ACKNOWLEDGMENTS

This work was supported by grants from the National Natural Science Foundation of China (no. 30971225 to L.Z.), the Specialized Research Fund for the Doctoral Program of Higher Education of China (no. 20111202110011 to L.Z.), and the Key Project of Science Technology (no. 206008 to L.Z.) from China Education Ministry.

The authors deeply appreciate the help of foreign expert Linda Perkins at Tianjin Medical University for critical reading of the manuscript and of Guangming Zhong (Department of Microbiology and Immunology, University of Texas Health Science Center at San Antonio, San Antonio, TX) for his gift of the *C. pneumoniae* polyclonal antibody.

The authors have no conflicts of interests.

REFERENCES

1. **Ross R.** 1999. Atherosclerosis—an inflammatory disease. N. Engl. J. Med. **340:**115e26.
2. **Schmidt R, Redecke V, Breitfeld Y, Wantia N, Miethke T, Massberg S, Fischel S, Neumann FJ, Schömig A, May AE.** 2006. EMMPRIN (CD 147) is a central activator of extracellular matrix degradation by *Chlamydia pneumoniae*-infected monocytes, implications for plaque rupture. Thromb. Haemost. **95:**151–158.
3. **Saikku P, Leinonen M, Mattila K, Ekman MR, Nieminen MS, Mäkelä PH, Huttunen JK, Valtonen V.** 1988. Serological evidence of an association of a novel *Chlamydia*, TWAR, with chronic coronary heart disease and acute myocardial infarction. Lancet **ii:**983–986.
4. **Zhang LJ, Zhang LJ, Quan W, Wang BB, Shen BL, Zhang TT, Kang Y.** 2011. Berberine inhibits HEp-2 cell invasion induced by *Chlamydophila pneumoniae* infection. J. Microbiol. **49:**834–840.
5. **Zhang L, Li X, Zhang L, Wang B, Zhang T, Ye J.** 2012. *Chlamydophila* (*Chlamydia*) *pneumoniae* infection promotes vascular smooth muscle cell adhesion and migration through IQ domain GTPase-activating protein 1. Microb. Pathog. **53:**207–213.
6. **Medzhitov R, Preston-Hurlburt P, Janeway CA, Jr.** 1997. A human homologue of the *Drosophila* toll protein signals activation of adaptive immunity. Nature **388:**394–397.
7. **Aderem A, Ulevitch RJ.** 2000. Toll-like receptors in the induction of the innate immune response. Nature **406:**782–787.
8. **Satta N, Kruithof EK, Fickentscher C, Dunoyer-Geindre S, Boehlen F, Reber G, Burger D, de Moerloose P.** 2011. Toll-like receptor 2 mediates the activation of human monocytes and endothelial cells by antiphospholipid antibodies. Blood **117:**5523–5531.
9. **Yang X, Coriolan D, Schultz K, Golenbock DT, Beasley D.** 2005. Toll-like receptor 2 mediates persistent chemokine release by *Chlamydia pneumoniae*-infected vascular smooth muscle cells. Arterioscler. Thromb. Vasc. Biol. **25:**2308–2314.
10. **Oh JY, Choi H, Lee RH, Roddy GW, Ylöstalo JH, Wawrousek E, Prockop DJ.** 2012. Identification of the HSPB4/TLR2/NF-κB axis in macrophage as a therapeutic target for sterile inflammation of the cornea. EMBO Mol. Med. **4:**435–448.
11. **Saber T, Veale DJ, Balogh E, McCormick J, NicAnUltaigh S, Connolly M, Fearon U.** 2011. Toll-like receptor 2 induced angiogenesis and invasion is mediated through the Tie2 signalling pathway in rheumatoid arthritis. PLoS One **6:**e23540. doi:10.1371/journal.pone.0023540.
12. **Sawa Y, Tsuruga E, Iwasawa K, Ishikawa H, Yoshida S.** 2008. Leukocyte adhesion molecule and chemokine production through lipoteichoic acid recognition by toll-like receptor 2 in cultured human lymphatic endothelium. Cell Tissue Res. **333:**237–252.
13. **Chun J, Prince A.** 2009. TLR2-induced calpain cleavage of epithelial junctional proteins facilitates leukocyte transmigration. Cell Host Microbe **5:**47–58.
14. **Chin YR, Toker A.** 2011. Akt isoform-specific signaling in breast cancer: uncovering an anti-migratory role for paladin. Cell Adh. Migr. **5:**211–214.
15. **Alessi DR, James SR, Downes CP, Holmes AB, Gaffney PR, Reese CB, Cohen P.** 1997. Characterization of a 3-phosphoinositide-dependent protein kinase which phosphorylates and activates protein kinase Balpha. Curr. Biol. **7:**261–269.
16. **Yang L, Qiao G, Ying H, Zhang J, Yin F.** 2010. TCR-induced Akt serine 473 phosphorylation is regulated by protein kinase C-alpha. Biochem. Biophys. Res. Commun. **400:**16–20.
17. **Zhang L, Teng Y, Zhang Y, Liu J, Xu L, Qu J, Hou K, Yang X, Liu Y, Qu X.** 2012. C-Src-mediated RANKL-induced breast cancer cell migration by activation of the ERK and Akt pathway. Oncol. Lett. **3:**395–400.
18. **Lang Y, Chen D, Li D, Zhu M, Xu T, Zhang T, Qian W, Luo Y.** 2012. Luteolin inhibited hydrogen peroxide-induced vascular smooth muscle cells proliferation and migration by suppressing the Src and Akt signalling pathways. J. Pharm. Pharmacol. **64:**597–603.
19. **Jung F, Haendeler J, Goebel C, Zeiher AM, Dimmeler S.** 2000. Growth factor-induced phosphoinositide 3-OH kinase/Akt phosphorylation in smooth muscle cells: induction of cell proliferation and inhibition of cell death. Cardiovasc. Res. **48:**148–157.
20. **Sandirasegarane L, Kester M.** 2001. Enhanced stimulation of Akt-3/protein kinase B-gamma in human aortic smooth muscle cells. Biochem. Biophys. Res. Commun. **283:**158–163.
21. **Chan KC, Wu CH, Huang CN, Lan KP, Chang WC, Wang CJ.** 2012. Simvastatin inhibits glucose-stimulated vascular smooth muscle cell migration involving increased expression of RhoB and a block of Ras/Akt signal. Cardiovasc. Ther. **30:**75–84.
22. **Hsieh HL, Wang HH, Wu CY, Tung WH, Yang CM.** 2010. Lipoteichoic acid induces matrix metalloproteinase-9 expression via transactivation of PDGF receptors and NF-kappaB activation in rat brain astrocytes. Neurotox. Res. **17:**344–359.
23. **Park DW, Lee HK, Jeong TW, Kim JS, Bae YS, Chin BR, Baek SH.** 2012. The JAK2-Akt-glycogen synthase kinase-3β signaling pathway is involved in toll-like receptor 2-induced monocyte chemoattractant protein-1 regulation. Mol. Med. Report. **5:**1063–1067.
24. **He X, Mekasha S, Mavrogiorgos N, Fitzgerald KA, Lien E, Ingalls RR.** 2010. Inflammation and fibrosis during *Chlamydia pneumoniae* infection is regulated by IL-1 and the NLRP3/ASC inflammasome. J. Immunol. **184:**5743–5754.
25. **Yaraei K, Campbell LA, Zhu X, Liles WC, Kuo CC, Rosenfeld ME.** 2005. Effect of *Chlamydia pneumoniae* on cellular ATP content in mouse macrophages: role of Toll-like receptor 2. Infect. Immun. **73:**4323–4326.
26. **Mukhopadhyay S, Clark AP, Sullivan ED, Miller RD, Summersgill JT.** 2004. Detailed protocol for purification of *Chlamydia pneumoniae* elementary bodies. J. Clin. Microbiol. **42:**3288–3290.
27. **Furness G, Graham DM, Reeve P.** 1960. The titration of trachoma and inclusion blennorrhoea viruses in cell cultures. J. Gen. Microbiol. **23:**613–619.
28. **Rödel J, Woytas M, Groh A, Schmidt KH, Hartmann M, Lehmann M, Straube E.** 2000. Production of basic fibroblast growth factor and interleukin 6 by human smooth muscle cells following infection with *Chlamydia pneumoniae*. Infect. Immun. **68:**3635–3641.

29. **Bhushan S, Tchatalbachev S, Klug J, Fijak M, Pineau C, Chakraborty T, Meinhardt A.** 2008. Uropathogenic *Escherichia coli* block MyD88-dependent and activate MyD88-independent signaling pathways in rat testicular cells. J. Immunol. **180:**5537–5547.
30. **Cai WJ, Wang MJ, Moore PK, Jin HM, Yao T, Zhu YC.** 2007. The novel proangiogenic effect of hydrogen sulfide is dependent on Akt phosphorylation. Cardiovasc. Res. **76:**29–40.
31. **Christine A. Petersen, Katherine A. Krumholz, Barbara A. Burleigh.** 2005. Toll-like receptor 2 regulates interleukin-1β-dependent cardiomyocyte hypertrophy triggered by *Trypanosoma cruzi*. Infect. Immun. **73:** 6974–6980.
32. **Barragán M, de Frias M, Iglesias-Serret D, Campàs C, Castaño E, Santidrián AF, Coll-Mulet L, Cosialls AM, Domingo A, Pons G, Gil J.** 2006. Regulation of Akt/PKB by phosphatidylinositol 3-kinase-dependent and -independent pathways in B-cell chronic lymphocytic leukemia cells: role of protein kinase C beta. J. Leukoc. Biol. **80:**1473–1479.
33. **MacIntyre A, Abramov R, Hammond CJ, Hudson AP, Arking EJ, Little CS, Appelt DM, Balin BJ.** 2003. *Chlamydia pneumoniae* infection promotes the transmigration of monocytes through human brain endothelial cells. J. Neurosci. Res. **71:**740–750.
34. **Uriarte SM, Molestina RE, Miller RD, Bernabo J, Farinati A, Eiguchi K, Ramirez JA, Summersgill JT.** 2004. Effects of fluoroquinolones on the migration of human phagocytes through *Chlamydia pneumoniae*-infected and tumor necrosis factor alpha-stimulated endothelial cells. Antimicrob. Agents Chemother. **48:**2538–2543.
35. **Mackern-Oberti JP, Maccioni M, Cuffini C, Gatti G, Rivero VE.** 2006. Susceptibility of prostate epithelial cells to *Chlamydia muridarum* infection and their role in innate immunity by recruitment of intracellular Toll-like receptors 4 and 2 and MyD88 to the inclusion. Infect. Immun. **74:**6973–6981.
36. **Coombes BK, Mahony JB.** 2002. Identification of MEK- and phosphoinositide 3-kinase-dependent signalling as essential events during *Chlamydia pneumoniae* invasion of HEp2 cells. Cell Microbiol. **4:**447–460.
37. **Wantia N, Rodriguez N, Cirl C, Ertl T, Dürr S, Layland LE, Wagner H, Miethke T.** 2011. Toll-like receptors 2 and 4 regulate the frequency of IFN-γ-producing $CD4^+$ T-cells during pulmonary infection with *Chlamydia pneumoniae*. PLoS One **6:**e26101. doi:10.1371/journal.pone.0026101.
38. **Borel N, Summersgill JT, Mukhopadhyay S, Miller RD, Ramirez JA, Pospischil A.** 2008. Evidence for persistent *Chlamydia pneumoniae* infection of human coronary atheromas. Atherosclerosis **199:**154–161.
39. **Park HD, Lee Y, Oh YK, Jung JG, Park YW, Myung K, Kim KH, Koh SS, Lim DS.** 2011. Pancreatic adenocarcinoma upregulated factor promotes metastasis by regulating TLR/CXCR4 activation. Oncogene **30:** 201–211.
40. **Yang HZ, Cui B, Liu HZ, Mi S, Yan J, Yan HM, Hua F, Lin H, Cai WF, Xie WJ, Lv XX, Wang XX, Xin BM, Zhan QM, Hu ZW.** 2009. Blocking TLR2 activity attenuates pulmonary metastases of tumor. PLoS One **4:**e6520. doi:10.1371/journal.pone.0006520.
41. **West XZ, Malinin NL, Merkulova AA, Tischenko M, Kerr BA, Borden EC, Podrez EA, Salomon RG, Byzova TV.** 2010. Oxidative stress induces angiogenesis by activating TLR2 with novel endogenous ligands. Nature **467:**972–976.
42. **Lasunskaia EB, Campos MN, de Andrade MR, Damatta RA, Kipnis TL, Einicker-Lamas M, Da Silva WD.** 2006. Mycobacteria directly induce cytoskeletal rearrangements for macrophage spreading and polarization through TLR2-dependent PI3K signaling. J. Leukoc. Biol. **80:**1480–1490.
43. **Fernández-Hernando C, József L, Jenkins D, Di Lorenzo A, Sessa WC.** 2009. Absence of Akt1 reduces vascular smooth muscle cell migration and survival and induces features of plaque vulnerability and cardiac dysfunction during atherosclerosis. Arterioscler. Thromb. Vasc. Biol. **29:**2033–2040.
44. **Seo J, Lee HS, Ryoo S, Seo JH, Min BS, Lee JH.** 2011. Tangeretin, a citrus flavonoid, inhibits PGDF-BB-induced proliferation and migration of aortic smooth muscle cells by blocking AKT activation. Eur. J. Pharmacol. **673:**56–64.
45. **Hirai I, Ebara M, Nakanishi S, Yamamoto C, Sasaki T, Ikuta K, Yamamoto Y.** 2012. Jurkat cell proliferation is suppressed by *Chlamydia* (*Chlamydophila*) *pneumoniae* infection accompanied with attenuation of phosphorylation at Thr 389 of host cellular p70S6K. Immunobiology **218:** 527–532.
46. **Lin FY, Lin YW, Huang CY, Chang YJ, Tsao NW, Chang NC, Ou KL, Chen TL, Shih CM, Chen YH.** 2011. GroEL1, a heat shock protein 60 of *Chlamydia pneumoniae*, induces lectin-like oxidized low-density lipoprotein receptor 1 expression in endothelial cells and enhances atherogenesis in hypercholesterolemic rabbits. J. Immunol. **186:**4405–4414.
47. **Walker L, Millena AC, Strong N, Khan SA.** 2013. Expression of TGFβ3 and its effects on migratory and invasive behavior of prostate cancer cells: involvement of PI3-kinase/AKT signaling pathway. Clin. Exp. Metastasis **30:**13–23.
48. **Shen Y, Kawamura I, Nomura T, Tsuchiya K, Hara H, Dewamitta SR, Sakai S, Qu H, Daim S, Yamamoto T, Mitsuyama M.** 2010. Toll-like receptor 2- and MyD88-dependent phosphatidylinositol 3-kinase and Rac1 activation facilitates the phagocytosis of *Listeria monocytogenes* by murine macrophages. Infect. Immun. **78:**2857–2867.
49. **Chen F, Zhu HH, Zhou LF, Wu SS, Wang J, Chen Z.** 2010. IQGAP1 is overexpressed in hepatocellular carcinoma and promotes cell proliferation by Akt activation. Exp. Mol. Med. **42:**477–483.